Supporting Information:

Structure and polymerization of liquid sulfur across the λ-transition

[1]

Manyi Yang,[†] Enrico Trizio,[†,‡] and Michele Parrinello[*,†]

†*Atomistic Simulations, Italian Institute of Technology, 16156 Genova, Italy*

‡*Department of Materials Science, Università di Milano-Bicocca, 20126 Milano Italy*

E-mail: michele.parrinello@iit.it

—————————————————

*The first and second authors contributed equally to this paper.

Table-of-contents

Supplementary Discussion

Radial distribution function and structure factor

In the main text, we report the $g(r)$ and the $s(k)$ for different ring concentrations generated with a *synthetic* approach starting from the same quantities computed for the pure phases in larger cells of 3456 atoms. To validate this approach, we report in Fig. S1 these quantities computed from simulations at the corresponding concentrations on a smaller cell of 512 atoms. It is evident that the two results are almost indistinguishable.
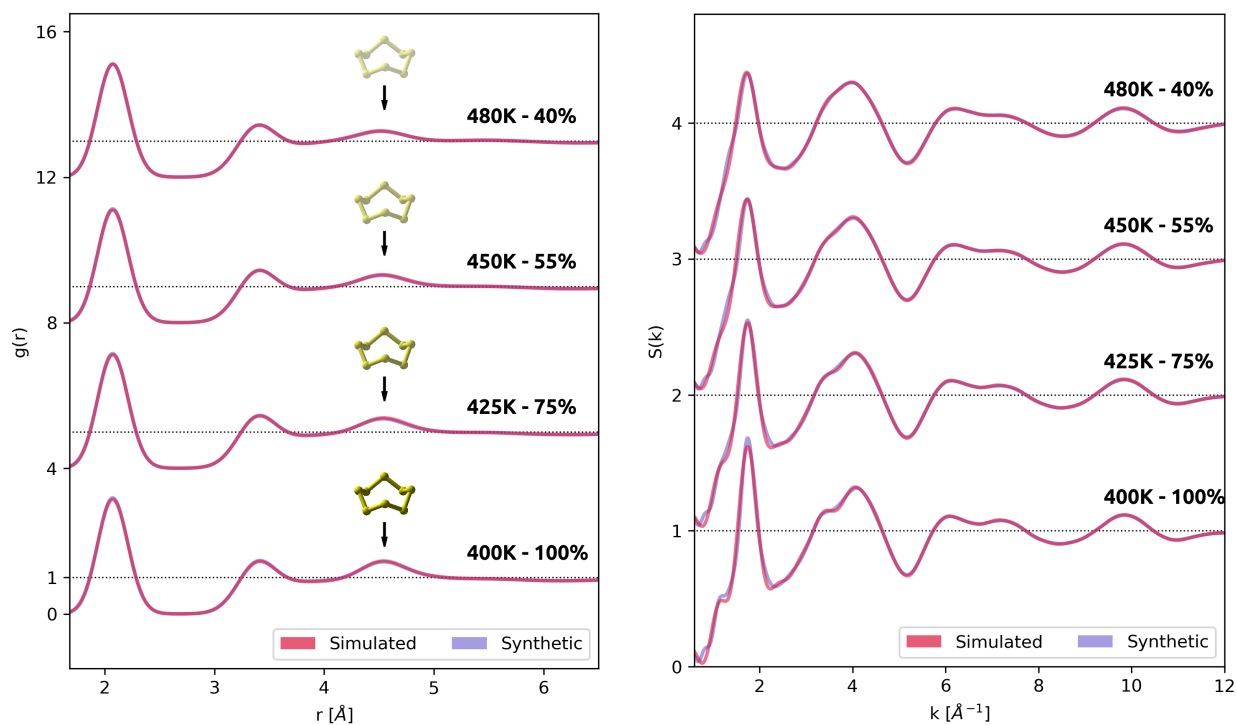
Supplementary Figure S1: Comparison of the radial distribution function and structure factor obtained using the approach reported in the main text for a 3456 atoms system and from unbiased simulations at the corresponding concentration of rings with a 512 atoms simulation cell.

14 In Fig. S2, we also report the $g(r)$ curves reported in the main text with and without the application of a Gaussian filter.
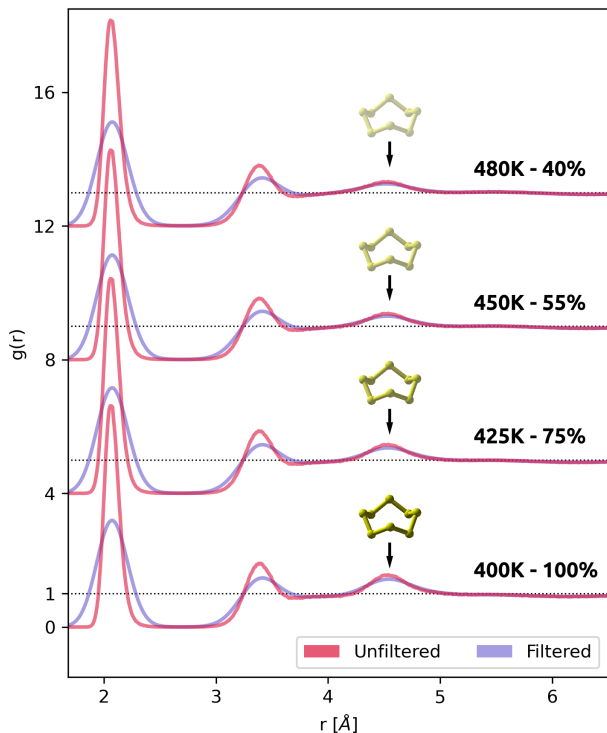
Supplementary Figure S2: Comparison of the radial distribution function before and after the application of the Gaussian filtering.

15

Validation of the NN potential

16

17 The mean absolute error (MAE) of energies in the training and test set are 1.92 and 0.66

18 meV/atom, respectively. The MAE of forces in the training and test set are 71.35 and 42.55

19 meV/Å, respectively (see Fig. S3) The test set was composed of roughly 10,000 atomic con-

20 figurations collected from both the unbiased simulations for polymer and molecular phases,

21 as well as from the biased simulations in which the active process of the polymerization of S_8

22 sulfur and its reverse were observed. These simulations were performed using our final NN

23 potential model on systems made of 512 atoms. The temperature was set to $432 \sim 500$ K,

24 and the simulation box was set to 24.8 Å to be consistent with the experimental densities.

25 The comparison of the DFT and NN predicted energies and atomic forces over the training

26 set and the test set are given in Fig.S3. It is not strange that the MAE of the training set
27 is larger than that of the test set because many active configurations in high temperature
28 and pressure ranges were included in the training set, which thus displays a broader range
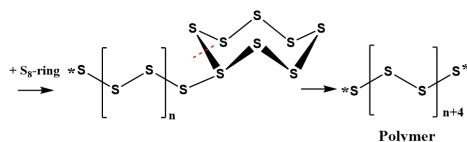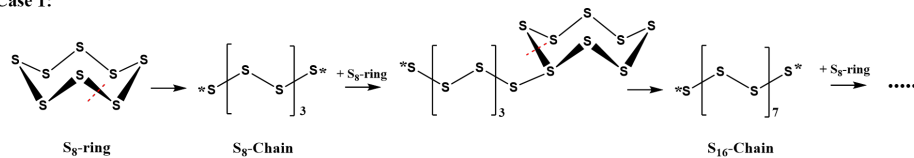29 of energies and forces distribution.
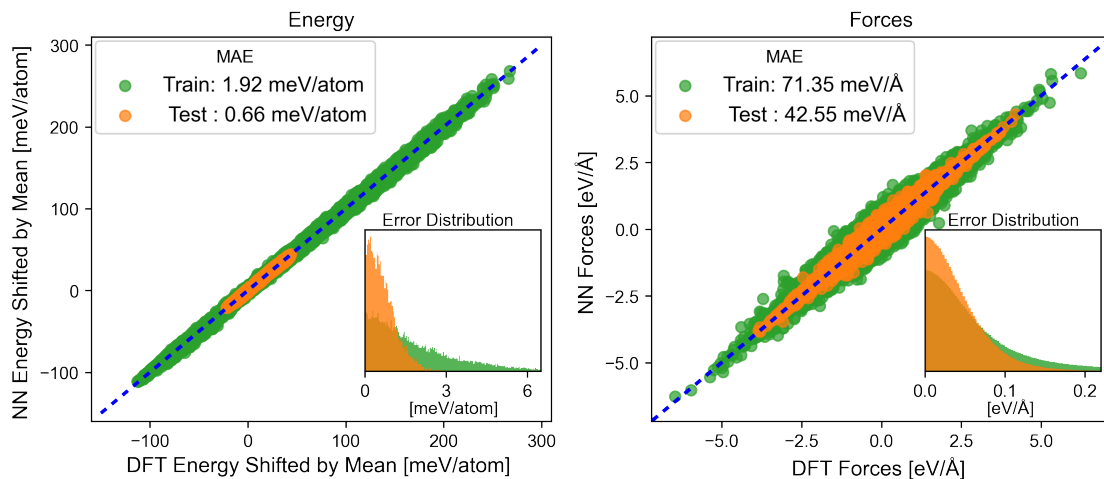
Supplementary Figure S3: Comparison of the energies (left panel) and atomic forces (right panel) calculated on the training set (green) and test set (orange) using DFT and the final NN potential. Energies in the left panel are shifted by the mean value of the DFT atomic energies. Insets illustrate the probability distributions of the absolute difference in energies and forces between the DFT and final NN model
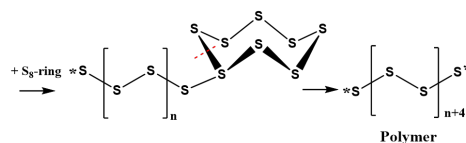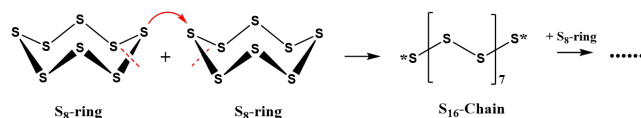
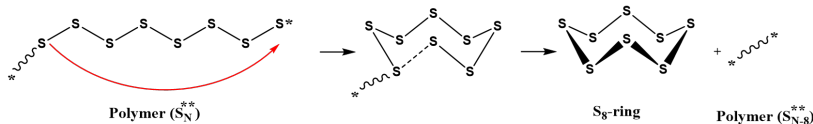# Supplementary Figures

Ring-opening Polymerization:
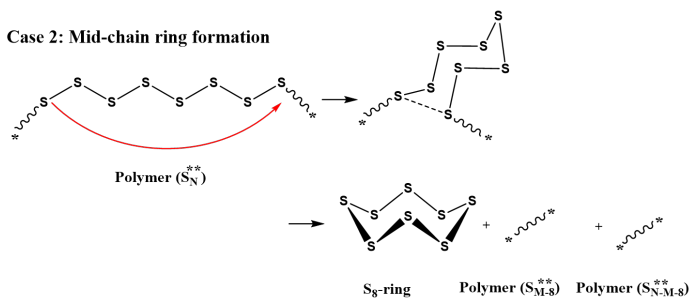
Case 1:

Case 2:
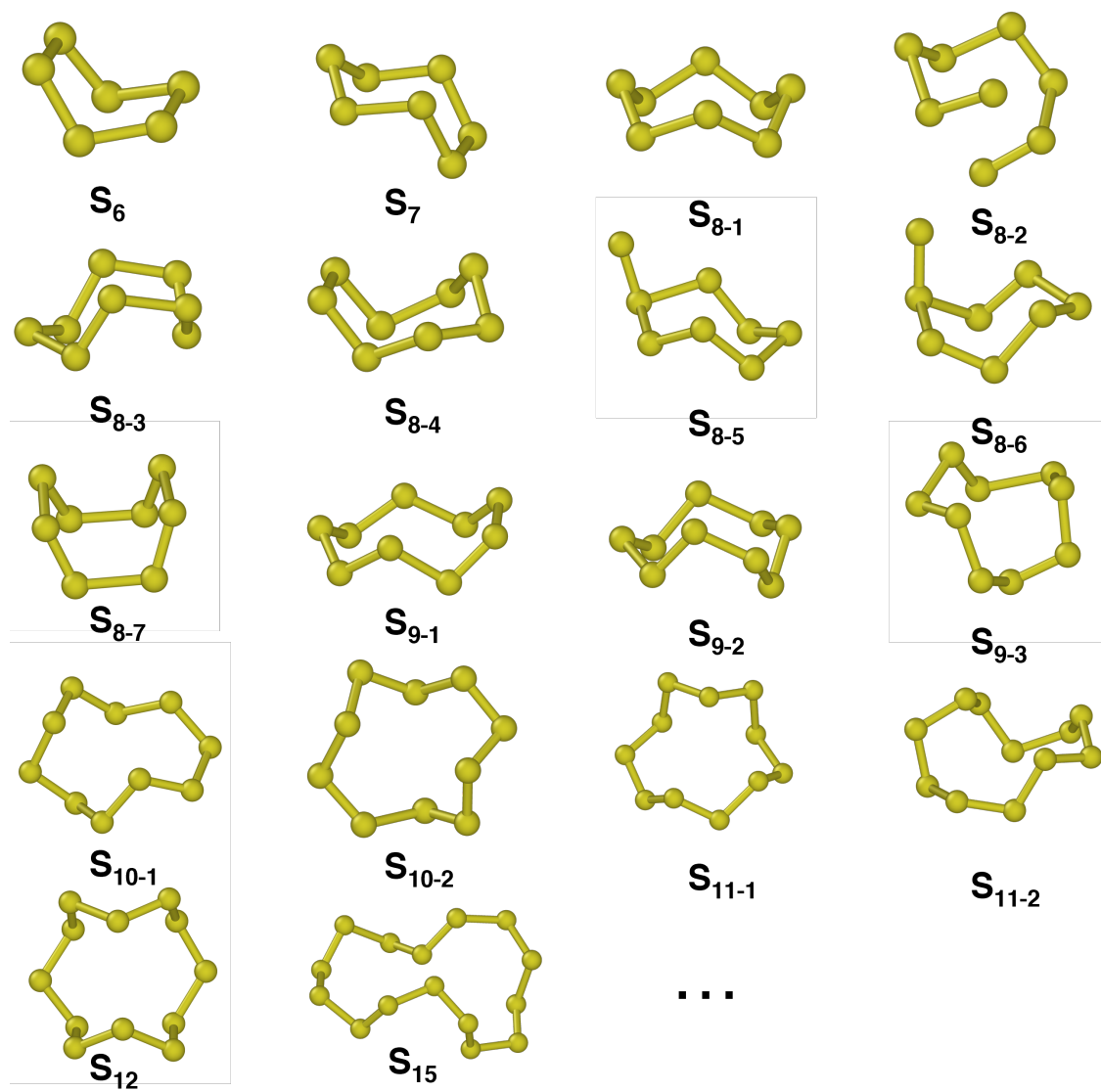

Ring-formation:

**Case 1: Chain tail ring formation**

Case 2: Mid-chain ring formation

Supplementary Figure S4: Schematic chemical representation of the polymerization and depolymerization mechanisms described in the main text.

S$_6$ **S$_7$**   **S$_{8-1}$**   **S$_{8-2}$**

S$_{8-3}$ **S$_{8-4}$**   **S$_{8-5}$**   **S$_{8-6}$**

S$_{8-7}$ **S$_{9-1}$**   **S$_{9-2}$**   **S$_{9-3}$**

S$_{10-1}$ **S$_{10-2}$**   **S$_{11-1}$**   **S$_{11-2}$**

S$_{12}$ **S$_{15}$**   . . .

Supplementary Figure S5: Snapshots of typical cyclic configurations ($6 < n < 15$) observed in our simulations. Such configurations were already reported in the literature and validated with DFT calculations. See Ref.[S1] and the references hereby.
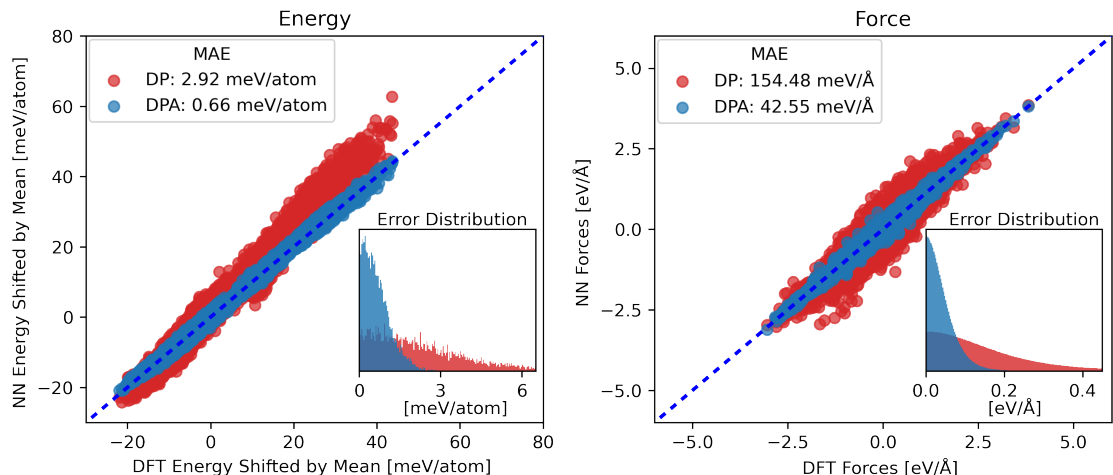
Supplementary Figure S6: Comparison of energies (left panel) and atomic forces (right panel) calculated on the test set using DFT and NN potentials trained with the Attention-based Deep Potential scheme (DPA, blue) and the standard Deep Potential-Smooth Edition scheme(DP, red). Energies in the left panel are shifted by the mean value of the DFT atomic energies. Insets illustrate the probability distributions of the absolute difference in energies and forces between the DFT and NN models. For the standard DP potential, we trained on the same training set as that of our final NN potential (DPA), as well as the same hyperparameters except for increasing the training steps from 3×10^6 to 5×10^6. The test is the same as that used to validate our final NN potential.

Supplementary References

(S1) Steudel, R. *Elemental sulfur and sulfur-rich compounds I*; Springer Science & Business Media, 2003; Vol. 2.